Spectral Partitioning and Identification of Wind Sea and Swell

JESÚS PORTILLA

Hydraulics Laboratory, Katholieke Universiteit Leuven, Heverlee, Belgium

FRANCISCO J. OCAMPO-TORRES

Departamento de Oceanografía Física, CICESE, Ensenada, Mexico

JAAK MONBALIU

Hydraulics Laboratory, Katholieke Universiteit Leuven, Heverlee, Belgium

(Manuscript received 6 October 2007, in final form 5 June 2008)

ABSTRACT

In this paper, different partitioning techniques and methods to identify wind sea and swell are investigated, addressing both 1D and 2D schemes. Current partitioning techniques depend largely on arbitrary parameterizations to assess if wave systems are significant or spurious. This makes the implementation of automated procedures difficult, if not impossible, to calibrate. To avoid this limitation, for the 2D spectrum, the use of a digital filter is proposed to help the algorithm keep the important features of the spectrum and disregard the noise. For the 1D spectrum, a mechanism oriented to neglect the most likely spurious partitions was found sufficient for detecting relevant spectral features. Regarding the identification of wind sea and swell, it was found that customarily used methods sometimes largely differ from one another. Evidently, methods using 2D spectra and wind information are the most consistent. In reference to 1D identification methods, attention is given to two widely used methods, namely, the steepness method used operationally at the National Data Buoy Center (NDBC) and the Pierson–Moskowitz (PM) spectrum peak method. It was found that the steepness method systematically overestimates swell, while the PM method is more consistent, although it tends to underestimate swell. Consistent results were obtained looking at the ratio between the energy at the spectral peak of a partition and the energy at the peak of a PM spectrum with the same peak frequency. It is found that the use of partitioning gives more consistent identification results using both 1D and 2D spectra.

1. Introduction

An ocean wave spectrum describes the distribution of the total wave variance over frequency and direction. Such a distribution is the result of the occurrence of a certain number of individual wave systems originating from different meteorological events. For the interpretation and archival of large datasets, integral parameters rather than whole spectra are preferred. However, while integral parameters suitably describe a wave spectrum composed of a unique wave system, the simultaneous occurrence of different wave systems turns integral parameters less meaningful, unless they refer to individual wave components. Partitioning of wave spectra into independent wave systems provides an excellent tool for data reduction. Also for the comparison of datasets or when evaluating model performance, the analysis at the level of wave systems gives more insight into processes than the analysis of mean parameters of the whole spectrum. For data assimilation purposes, the use of spectral partitioning has given rise to the development of more robust sequential algorithms (Hasselmann et al. 1996; Young and Glowacki 1996; Voorrips et al. 1997), because previous sequential schemes had faced constraints at the moment of updating the spectrum as there is no reason to change the partial contribution of each individual system in the absence of additional information (Thomas 1988; Lionello et al. 1992). Additionally, spectral components can be associated in space and time to trace the evolution of wave systems originating from remote storms (Hanson and Phillips 2001; Quentin 2002).

Corresponding author address: Jesús Portilla, K.U. Leuven, Kasteelpark Arenberg 40, Postbus 2448, 3001 Heverlee, Belgium.
E-mail: jesus.portilla@bwk.kuleuven.be

DOI: 10.1175/2008JTECHO609.1

One of the potential applications of partitioning in third-generation wave modeling is the determination of wind sea and swell. As these components are no longer computed separately, and model users have traditionally disposed of such information, there is a need for splitting the spectrum to provide this information as part of the output products (Bidlot 2001). On the other hand, in wave studies where the identification of wind sea and swell is relevant, nearly each author has adopted his/her own criteria based on some physical properties of wind and waves, and therefore several methods can be found in the literature (Wang and Hwang 2001; Violante-Carvalho et al. 2002).

For consistency, in the rest of the paper, *partitioning* will be seen as the mechanism to detect wave systems looking at morphological features of the spectral signature only. *Identification*, on the other hand, refers to labeling with wind sea or swell as a supplementary designation taking into account environmental and physical characteristics.

For the present study, different partitioning–identification schemes available in the literature have been implemented and compared. The description of the different methods has been structured in two main blocks, the first considering partitioning methods only (section 2) and the second considering the identification step (section 3). Within each of these two blocks, 2D and 1D schemes are treated. The analysis points at strengths and shortcomings, and wherever possible, a more robust scheme is proposed. Examples at the end of each section illustrate the findings.

2. Partitioning methods

a. 2D partitioning schemes

The first conceptual partitioning algorithm was presented by Gerling (1992). In his algorithm, the lowest energy threshold value at which upper parts of the spectrum get disconnected is found. This process is repeated until all systems are detected. To determine whether partitions are significant, integral mean parameters are compared with spectral components of neighboring points and subsequent times (pattern-extraction algorithm). A partition is considered significant if it is persistent in time and space.

Many partitioning schemes (e.g., Hanson and Phillips 2001; Voorrips et al. 1997) are specific implementations of the scheme described by Hasselmann et al. (1996). The basic idea of this scheme is the same as that of Gerling (1992), although the concept of the algorithm differs slightly. According to Hasselmann et al. (1996), a wave spectrum can be regarded as an inverted catchment area, making an analogy with hydrological concepts (see also Brüning et al. 1994; Hasselmann et al. 1994). The different subcatchments of that main catchment area are determined by associating each spectral grid point to a unique neighbor, namely, the one with the highest energy level. Grid points corresponding to the same local peak are clustered, and each of these clusters defines a partition (watershed algorithm). To assess the significance of the partitions, some of their morphological characteristics are intercompared. In Hasselmann et al. (1996), two partitions are merged into one:

- if two peaks are one grid cell apart,
- if the trough between them is not sufficiently pronounced (i.e., the lowest point between two partitions is greater than 85% of the smaller peak), or
- if the square spectral distance between two peaks is shorter than the spread of any of the two systems (see Table 1 for definitions).

Other authors (e.g., Voorrips et al. 1997; Hanson and Phillips 2001) have used the scheme of Hasselmann et al. (1996) with different settings for the combining parameters. These implementations are briefly described in section 2a.

1) Discussion

Actually, partitioning results from the two methods above are similar. However, assessing whether those systems are significant is less straightforward. This is especially the case for observed spectra because these contain considerable random variability. Although model spectra do not contain such random variability, assessing the significance of partitions will become more problematic as spectral resolution increases.

Gerling's (1992) approach is consistent if several observations of the same network, or model spectra, are

TABLE 1. Summary of parameters for combining partitions in the 2D spectrum according to different implementations.

	Low energy threshold	Contrast	$\Delta f^2/\delta f^{2}$*
Hasselmann et al. (1996)	—	0.85	1
Voorrips et al. (1997)	0.0025 m^2	0.70	0.5
Hanson and Phillips (2001)	$e \le A/(f_p^4 + B)$**	0.65–0.75	0.4–0.5

*Squared distance of spectral peaks (1) and (2): $\Delta f^2 = (f_x^{(1)} - f_x^{(2)})^2 + (f_y^{(1)} - f_y^{(2)})^2$; $f_x = f\cos\theta$; $f_y = f\sin\theta$. Spectral spread: $\delta f^2 = \overline{(f_x - \overline{f_x})^2} + \overline{(f_y - \overline{f_y})^2}$; $\overline{f_x} = \overline{f\cos\theta}$; $\overline{f_y} = \overline{f\sin\theta}$.

** The wave system energy is denoted by e, f_p is peak frequency, and A and B are calibration parameters.

processed. In both cases, wave systems can be intercompared and their persistence can be assessed. A practical limitation is that it demands the availability of other spectra. Moreover, the number of partitions detectable in an observed spectrum is typically of the order of tens; thus, associating several wave components with neighboring components at different times becomes very, if not too, intricate. Gerling (1992) already pointed at this when he states: "It does not appear possible to obtain completely satisfactory results with the simple metric just defined."

Hasselmann et al.'s (1996) approach does not suffer from these limitations. In their scheme, spectral features are intercompared within the spectrum. However, the criteria used for merging partitions rely on rather arbitrary parameters that need to be adjusted from situation to situation. Moreover, different users of this scheme have adopted different parameters (Voorrips et al. 1997; Hanson and Phillips 2001). To this end, Hanson and Phillips (2001) suggested the need for an additional routine that optimizes the choice of the parameters by an iterative procedure. And they emphasized the need for removing partitions with energy under a threshold value determined by the spectral falloff given by Phillips (1985). However, it is not evident that those small partitions should actually be removed. Voorrips et al. (1997) simply merge partitions with low energy (i.e., lower than 0.0025 m^2). Table 1 summarizes the parameter settings for the different implementations described above.

While spectral partitioning is conceptually a robust and simple method, the need for continuous calibration becomes tedious, especially in operational or automated conditions. Moreover, inappropriate choice of combining parameters renders the method unstable and unreliable. The combining mechanism is crucial because it determines which partitions are significant and how those partitions are merged to determine the resulting wave systems. Similar remarks referring to the complexity of determining the significance of partitions have been pointed out before by Aarnes and Krogstad (2001).

2) PROPOSED 2D PARTITIONING ALGORITHM

The previous section pointed out that the calibration of the combining algorithm is the main difficulty in producing meaningful partitions. In general, adjusting parameters for one situation produces deficient results in others. This will be illustrated with example 1. In this paper, an image-processing tool is introduced in the combining algorithm, aimed at alleviation of the parameterization dependence. The 2D wave spectrum is thus treated as an image. As in many cases (either for observed or model spectra), the main problem is the presence of spurious partitions. A 2D noise-removal (smoothing) filter has been implemented and tested with satisfactory results. This filter consists of a 2D discrete convolution operation between the spectrum and an equally weighted convolution kernel that averages all immediate neighbors of a central bin. That operation is mathematically expressed as

$$\begin{aligned}\hat{S}(i,j) &= \kappa(m,n) \otimes S(i,j) \\ &= \sum_{m=-1}^{1}\sum_{n=-1}^{1} \kappa(m,n)S(i-m,j-n),\end{aligned} \qquad (1)$$

where $\hat{S}$ is the filtered spectrum and S is the raw spectrum, both having dimensions $i \times j$. The operator $\otimes$ indicates a convolution. The convolution kernel κ is chosen as a constant 3×3 matrix with coefficients summing to unity [i.e., $\kappa(m,n) = {}^{1}/_{9}, \forall\ m,n$].

Obviously, different possibilities exist for the choice of the kernel, and the spectral image might be subject to more elaborated image processing. However, a setup including this filter seems to perform well in most typical circumstances. Note that this filtering process can be repeated, and an important aspect to be addressed is to what extent the wave spectrum has to undergo repeated filtering. It is clear that more spurious partitions are present in observed spectra than in model spectra and will require more filtering. On the other hand, excessive filtering causes blurring, which may render patterns indiscernible. Two measures are taken to tackle this aspect: the first is to indicate a priori a number of expected significant systems in the spectrum, and the second is to merge partitions with low energy by setting a noise energy threshold (called *thresholding*).

The partitioning-combining method advocated in this paper is set up as follows:

1) the spectrum is partitioned with the watershed algorithm;
2) low-energy partitions are merged (thresholding);
3) if the number of partitions is higher than the prescribed number, the spectrum is filtered, partitioned, and low-energy partitions are merged (thresholding);
4) step 3 is repeated until the number of partitions detected is equal or lower than the prescribed number; and
5) low-energy partitions are merged (combining).

The degree of filtering is thus determined implicitly by the prescribed number of partitions and the noise threshold. Note that the thresholding (step 2) and the last combining due to low energy (step 5) are carried out by the same subroutine, but they are conceptually two

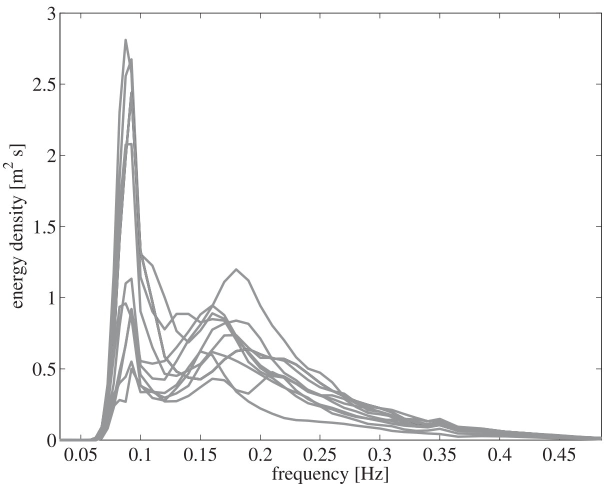

FIG. 1. 1D energy spectra from NDBC buoy 41013 (33°26′11″N, 77°44′35″W) from 0000 UTC 10 Apr 2006 to 0600 UTC 12 Apr 2006. Spectra are drawn every 6 h.

different operations. Thresholding aims at suppressing noise, because if the reduction of partitions is carried out by filtering alone, excessive filtering would be needed and the blurring effect would be stronger. The combining process aims to disregard small systems that are probably real systems but are not necessarily important. The thresholding-combining subroutine merges the target partition with the closest adjacent partition in the frequency-direction space. Tests in a number of different circumstances with buoy and model spectra suggested the following settings:

- number of expected partitions: between 4 and 6,
- energy level for noise thresholding: between 1% and 2% of the total energy in the spectrum, and
- energy level for last combining: between 5% and 8% of the total energy in the spectrum.

3) EXAMPLE 1

The 2D partitioning–combining procedures are illustrated using wave spectra from the National Buoy Data Center (NDBC) buoy 41013. The period from 0000 UTC 10 April 2006 to 0600 UTC 12 April 2006 was chosen. During this period, the wave conditions are characterized by double-peaked spectra, as shown in Fig. 1 (for clarity, 1D spectra are shown).

These spectra have been partitioned and combined according to the criteria of Hasselmann et al. (1996; Table 1) and also by using the combining algorithm proposed in this study (section 2a). Time series of wave energy and mean frequency are presented in Fig. 2. Note that to draw Fig. 2, partitions in consecutive spectra need to be numbered in a consistent manner. For all combinations of partitions of the current and the previous time step, the difference between the mean frequency is calculated. Combinations closest in mean frequency are assigned the same partition number.

Using Hasselmann et al.'s (1996) scheme, there is only one main partition most of the time (thin, continuous, circle-marked line in Fig. 2), although a second partition appears and disappears on some occasions. The mean parameters of the first partition are relatively

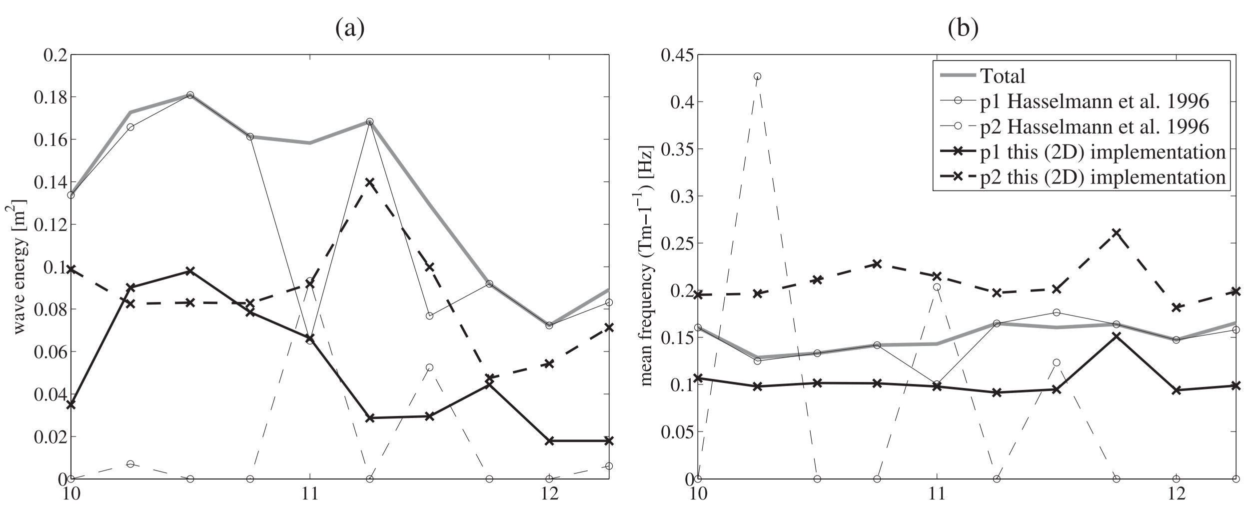

FIG. 2. Time series of (a) wave energy and (b) mean wave frequency (Tm^{-1}) for NDBC buoy 41013 (33°26′11″N, 77°44′35″W) for the period 0000 UTC 10 Apr 2006 to 0600 UTC 12 Apr 2006 for the whole spectrum (gray thick line). For partitions calculated with the Hasselmann et al. (1996) scheme: first partition (continuous circle-marked line) and second partition (dashed circle-marked line). Results from this study 2D implementation: first partition (thick continuous cross-marked line) and second partition (thick dashed cross-marked line).

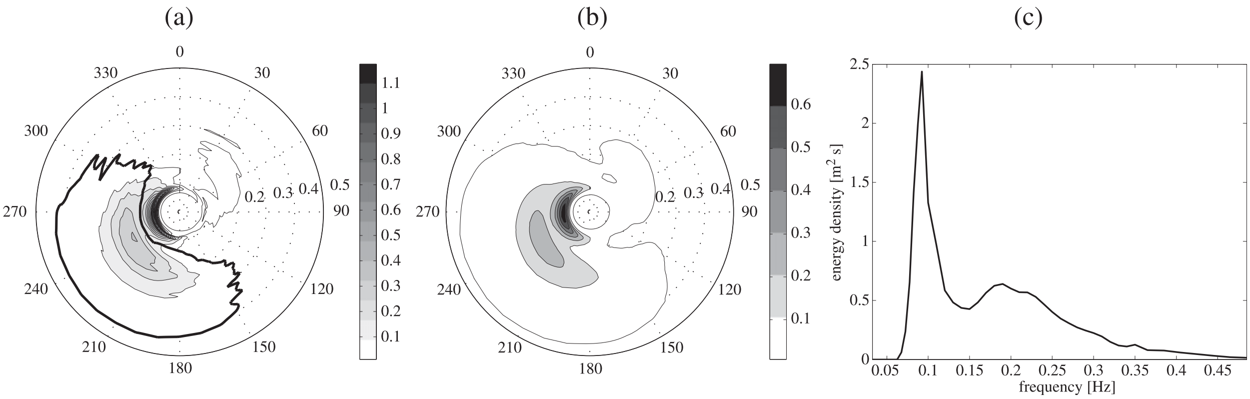

FIG. 3. Spectrum from NDBC buoy 41013 (33°26′11″N, 77°44′35″W) at 1800 UTC 10 Apr 2006. (a) 2D spectrum, (b) 2D smoothed spectrum, and (c) 1D spectrum.

stable and agree well with those of the total spectrum, while two systems are discernible from the spectra (Fig. 1). The mean parameters of the second partition look more like pure noise. The combining algorithm proposed here detects two wave systems as being equally significant. Their evolution in time is quite stable. This is in agreement with what it is expected from the spectra (Fig. 1).

To analyze details, the spectrum at 1800 UTC 10 April 2006 is shown in Fig. 3. Visual inspection indeed suggests that two main wave systems are present (note, in fact, that also a third one is distinguishable in the 2D spectrum, but its energy is much lower). To facilitate the discussion, one of these systems has been contoured (with a black thick line) in Fig. 3a.

The watershed algorithm detects 16 partitions in this spectrum. According to the Hasselmann et al. (1996) criteria, basically all systems are merged into one partition. The condition for which the two (indicated) main partitions are combined is that the square distance between the two peaks (i.e., 0.0088) is lower than the spread of either system (i.e., 0.0183 and 0.0259). On the other hand, according to the 2D implementation of Voorrips et al. (1997; see Table 1), the spectral peak distance must be lower than the 0.5 spread of either system, but even that condition is not yet sufficient to keep these two main systems uncombined. Alternatively, following Hanson and Phillips (2001) that distance must be lower than 0.4 the spread of either system. Although this factor seems appropriate in this case, these two partitions would be combined in a further step with their set of parameters because the trough between the two peaks (contrast) is required to be less than 0.65 the energy of the lower peak. The contrast level corresponds in this example to 0.67 which, on the other hand, satisfies Hasselmann et al.'s (1996) and Voorrips et al.'s (1997) contrast conditions (i.e., 0.85 and 0.70, respectively). Conveniently, one could choose other factors for this case (i.e., 0.4 for the spectral spread and 0.70 for the contrast) without guarantee that these factors will work for the other spectra.

Using the combining procedure proposed here alleviates the sensitivity to parameter settings and increases the ability of the method to detect relevant spectral features. For the present example, after the spectrum has been smoothed once (Fig. 3b), the watershed algorithm detects 5 partitions instead of 16. From those five partitions, three have energy lower than 2% of the total energy and are merged by the thresholding step; the low-energy combining threshold was set to 5%, but it does not operate in this particular spectrum. This results in the two main wave systems shown in Fig. 3a.

b. *1D partitioning schemes*

The 1D partitioning and combining scheme introduced by Voorrips et al. (1997) is a straightforward adaptation of the 2D scheme of Hasselmann et al. (1996). Similarly, each local peak represents the peak of a wave system. The minima between adjacent peaks constitute the partition limits. The combination of partitions is also done under similar criteria:

- if two peaks are within their spectral width (i.e., peaks are closer than half the width at half the maximum of either of the two peaks),
- if the trough between them is not sufficiently pronounced (i.e., the lowest point between two partitions is greater than 50% of the smaller peak), and
- if the partition energy is lower than a threshold (i.e., 0.0025 m^2).

Additionally, two extra conditions are adopted to detect significant partitions. The first aims at identifying mixed sea states by comparing the mean direction with peak direction of two potentially merging partitions to split them again. The second also considers wind information to combine all potential pure wind sea states. These two extra conditions should not (or cannot) be considered if no directional or wind information is available.

Rodríguez and Guedes Soares (1999) also presented a method to detect significant peaks. Taking into account the energy variability of the spectrum, they consider that some spurious peaks appear due to natural random fluctuations of the spectral estimates. Significant peaks lie outside the confidence interval of those estimates—that is, if the height of a peak, measured from the previous minimum, is greater than the width of the confidence band. The confidence interval is computed considering a chi-square distribution. The parameters of the chi-square distribution (i.e., number of degrees of freedom and the level of confidence) determine the magnitude of significant and spurious peaks.

Violante-Carvalho et al. (2002) presented another set of criteria to detect significant peaks:

- if two peaks are very close to each other (i.e., closer than twice the spectral resolution, 0.03 Hz),
- if the ratio between two adjacent peaks is lower than 15, and
- if the trough between them is not sufficiently pronounced (i.e., lower limit of the 90% confidence interval of the greater peak higher than the upper limit of the 90% confidence interval of the trough between the peaks).

1) Discussion

As in the case of the 2D spectrum, the combining mechanism is based on contrast and the ratio of peak square distance to spectral spread is deficient and depends strongly on the parameterizations. Therefore, the 1D combining algorithm of Voorrips et al. (1997) based on these criteria suffers of the same shortcomings associated with the 2D scheme of Hasselmann et al. (1996). Moreover, in the scheme of Violante-Carvalho et al. (2002), the comparison between energy levels of adjacent peaks and the magnitude of the trough between peaks are conditions analogous to the contrast criterion and have the same limitations.

Also the criterion of Rodríguez and Guedes Soares (1999) is similar to the contrast criterion. However, increasing the number of degrees of freedom of the spectrum has a similar effect as filtering. In that sense, this approach is consistent with the idea used in section 2a to improve the 2D scheme. However, the scheme of Rodríguez and Guedes Soares (1999) was not investigated further in this study, mainly because tests using a convolution function to smooth the 1D spectrum showed that the blurring effect was too aggressive in the case of the 1D spectrum. As a consequence, spectral patterns quickly became indiscernible, resulting in unsatisfactory overall performance of the scheme. Because the smoothing approach did not contribute to the improvement of the 1D algorithm, results are not presented here. However, satisfactory partitioning results were obtained by a mechanism aiming to combine the most likely spurious peaks. This scheme is presented in the next section.

2) Proposed 1D partitioning algorithm

To disregard the most likely spurious peaks and eventually concentrate efforts in detecting more complex features, a simple scheme was implemented. It turned out that once these (most likely spurious) peaks are disregarded, the so-determined partitions are rather consistent and these criteria are considered sufficient for the 1D combining mechanism. The procedure to detect peaks as spurious is as follows:

1) partitions having the peak frequency above a certain threshold (i.e., 0.35–0.4 Hz); the reason for this measure is that in the tail of the spectrum, usually high variability is present, which is very difficult to treat, while in reality peaks in the tail belong to the wind sea part;
2) partitions with low total energy (i.e., lower than 5%–8% of the total energy);
3) partitions having few spectral bins before or after the peak (i.e., less than 2 bins); and
4) partitions that are placed between two other (neighboring) partitions and have a lower peak energy level than these two neighbors.

3) Example 2

In the present example, the 1D partitioning–combining procedure of Voorrips et al. (1997) (without using wind or directional information) is compared to the 1D implementation given in this study (section 2b). The dataset is the same as that used in the illustration of the 2D scheme (Fig. 2). The resulting time series of the 1D partitioning for wave energy and mean frequency (Tm^{-1}) are shown in Figs. 4a,b, respectively.

As in the case of the 2D scheme (Hasselmann et al. 1996), one main wave system is detected using the 1D scheme of Voorrips et al. (1997) (thin continuous circle-marked line). This first partition contains most of the energy, and its main frequency agrees with that of the entire spectrum. A second partition appears sporadically. From the spectra (Fig. 1), two significant partitions are expected.

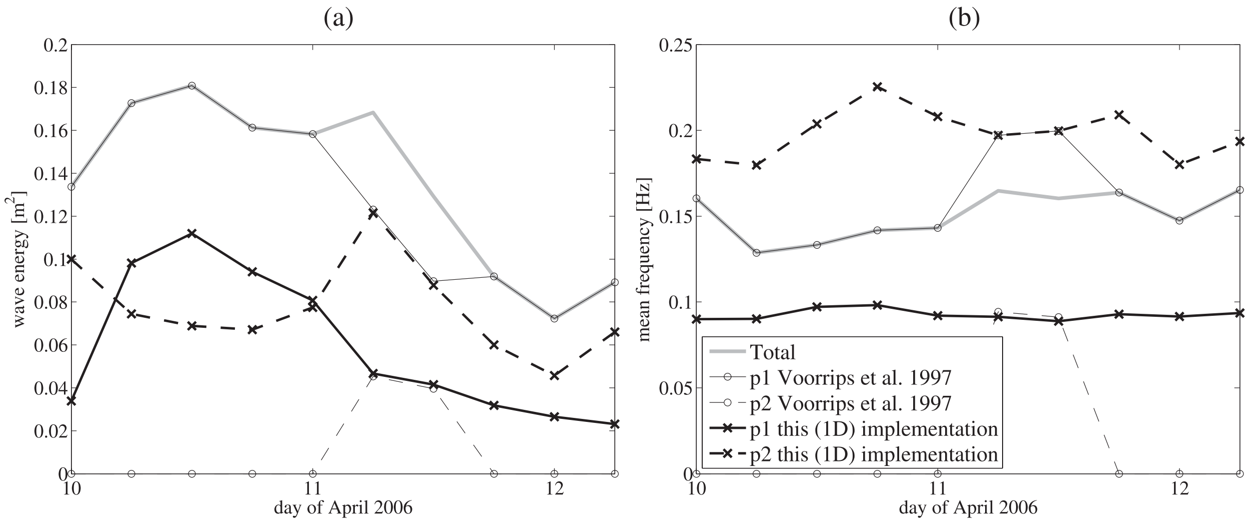

FIG. 4. Time series of (a) wave energy and (b) mean wave frequency (Tm^{-1}) for NDBC buoy 41013 (33°26′11″N, 77°44′35″W) for the period 0000 UTC 10 Apr 2006 to 0600 UTC 12 Apr 2006 for the whole spectrum (gray thick line). For partitions calculated with Voorrips et al. (1997) 1D scheme: first partition (continuous circle-marked line) and second partition (dashed circle-marked line). Results from this study 1D implementation: first partition (thick continuous cross-marked line) and second partition (thick dashed cross-marked line).

The 1D combining procedure outlined here detects the two systems present in the spectra. These time series are also quite consistent with the time series of the 2D scheme (Fig. 2). Obviously, certain differences exist between results of the 1D and the 2D schemes (i.e., 1800 UTC 11 April 2006), mainly because not all of the features that are visible in the 2D spectrum are also visible in the 1D spectrum. However, the evolution of the two systems is very similar.

3. Wind sea–swell identification methods

In section 2, the detection of different wave systems was done exclusively on the basis of morphological features. In this section, environmental and physical features are also regarded to assess the character of their meteorological origin. Locally generated waves growing actively under the influence of wind (wind sea) and remotely generated waves (swell) arriving to the measuring site are distinguished. Following Holthuijsen (2007), wind sea waves are more irregular and short crested, respond quickly to wind variations, and are characterized by a rather broad spectrum, while swell consists of rather regular long-crested waves whose evolution is not as strongly affected by wind. A swell spectrum is narrower, and as the wind drops or when waves leave the generation area, their steepness reduces sharply due to frequency-direction dispersion.

From a more practical point of view, the energy of wind sea waves is contained at higher frequencies (i.e., between about 0.1 and 4 Hz) while swell waves have lower frequencies (i.e., between 0.03 and about 0.2 Hz). In wave modeling, wind sea is the part of the spectrum subjected to a positive wind-input term (Bidlot 2001).

The distinction between wind sea and swell is often not obvious. Under changing winds (both magnitude and direction) wave systems can overlap in the frequency-direction domain, giving origin to a rather continuous spectrum in which the presence of two or more distinct systems is not clearly discernible. Wave systems in these situations are referred to as mixed sea states and are particularly difficult (if not impossible) to detect and/or identify by automated procedures.

It is evident that more objective and reliable identification algorithms can be constructed when the full 2D wave spectrum and the wind speed and direction are considered. In cases when only the 1D spectrum is available, extracting some extra information from it is also advantageous. In the following sections, different wind sea – swell identification methods reported in the literature are studied. Both 2D and 1D spectra are considered.

a. Wind sea–swell identification using 2D spectrum and wind data

If 2D spectrum and wind information are available, a straightforward step to identify wind sea and swell is to apply a definition for wind sea. Suitably, the definition from numerical modeling might be adopted, for which a wind wave generation formulation must be considered. In the wave model (e.g., WAM cycle VI; Komen et al. 1994), in particular, although the wind wave generation mechanism actually implemented is the one given by Janssen (1991), the identification of wind sea and swell

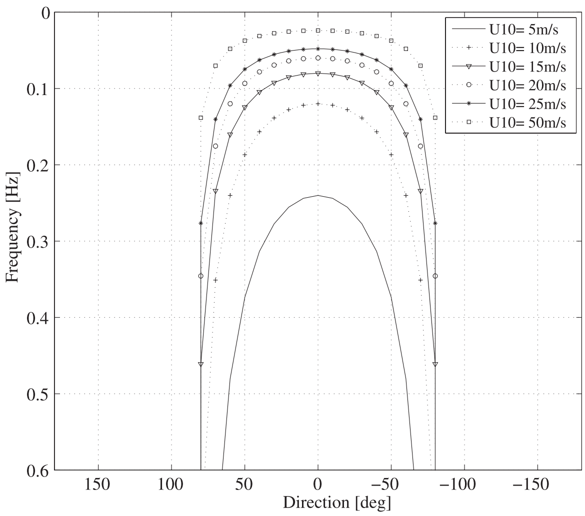

FIG. 5. Limit of wind sea and swell in the frequency-direction domain according to Eq. (2) for different values of wind speed (U_{10}) and $\beta = 1.3$. The wind sea area is under the curves.

is based on the formulation of Komen et al. (1984) [Eq. (2)]. While Janssen's (1991) mechanism takes into account the sea state to compute the wind input, Komen et al.'s (1984) formula simply defines a region in the 2D spectrum for the wind input (Fig. 5):

$$\beta \frac{U_z}{c_p} \cos(\theta - \psi) > 1, \tag{2}$$

where U_z is the wind velocity at height z, c_p is phase speed [i.e., $c_p = g/(2\pi f)$ in deep water], θ is the wave direction, ψ is the wind direction, g is the gravity acceleration, f is the wave frequency, and β is a calibration factor. Similar criteria based on wave age (U_z/c_p) are used by others to identify wind seas; see, for example, Donelan et al. 1985 and Drennan et al. 2003.

The magnitude of the factor β in Eq. (2) is not irrelevant, as it directly affects the extent of the wind sea area in the spectrum. A value of $\beta \leq 1.3$ has typically been applied to characterize the region of pure wind sea (Hasselmann et al. 1996; Voorrips et al. 1997; Bidlot 2001). Moreover, Hasselmann et al. (1996) consider old wind sea systems as those having the peak within the region where $1.3 < \beta \leq 2.0$. Additionally, to identify mixed sea states produced by a (fast) wind rotation, they impose that either the peak parameters or the mean parameters (frequency and direction) of a wave system must fulfill the old wind sea criterion.

1) DISCUSSION

In practice, Eq. (2) can be applied in either one of two ways: 1) by considering the partitioned 2D spectrum, in which case the phase velocity and direction are those of the peak (or mean) of the partition or 2) by not partitioning the spectrum, in which case each spectral grid point is evaluated independently by Eq. (2).

The disadvantage of applying Eq. (2) to each grid point is that the frequency-direction area that fits the wind sea–swell criterion (Fig. 5) does not necessarily correspond with a wave system and the spectrum is split even in situations in which the spectrum is composed of only one wave system. Not surprisingly, more consistent results in terms of wave systems are obtained if partitioning is used.

2) EXAMPLE 3

The difference between applying Eq. (2) to the partitioned and nonpartitioned spectra is illustrated, considering 6-hourly spectra from the European Centre for Medium-Range Weather Forecasts (ECMWF) Meteorological Archive and Retrieval System (MARS) archive (limited-area deterministic system WAM using the assimilation system) at Westhinder in the southern North Sea (51.50°N, 2.50°E) from 0000 UTC 26 January 2007 to 1800 UTC 31 January 2007. Note that the ECMWF WAM model applies Eq. (2) to each frequency-direction bin for identifying wind sea.

The ECMWF gives a continuous occurrence of swell (Fig. 6b) with a notorious peak at 1200 UTC 27 January, but with the support of partitioning there are two successive swell events: one at 1200 UTC 28 January and the second at 1200 UTC 29 January, originating from the two wind activity events (Fig. 6a). In any case, the ECMWF swell estimates are of larger magnitude. Also, maxima of swell energy are not occurring at the same time. For instance, for the first swell event, the ECMWF identification reaches its maximum 12 h earlier than when working with partitions. Note the evolution of the decaying wind sea system when partitioning is used. For example, the wind sea system present at 1200 UTC 27 January evolves from a pure wind sea into an old wind sea, then into a mixed wind sea (due to wind rotation from northwest to north) and finally into swell.

One can also follow the evolution of wave systems from looking at the time series of frequency and direction (Figs. 6c,d). While the swell frequencies from the ECMWF estimates are quite continuous and appear rather constant, the evolution of the systems also using partitions looks more episodic. For instance, in the swell event of 28 January starting at 1800 UTC, low- frequency swell waves arrive first. The swell mean frequency increases progressively. The energy in the swell systems from the two storm events decay faster (and even extinguish) than the ECMWF-assigned swell energy (Fig. 6b).

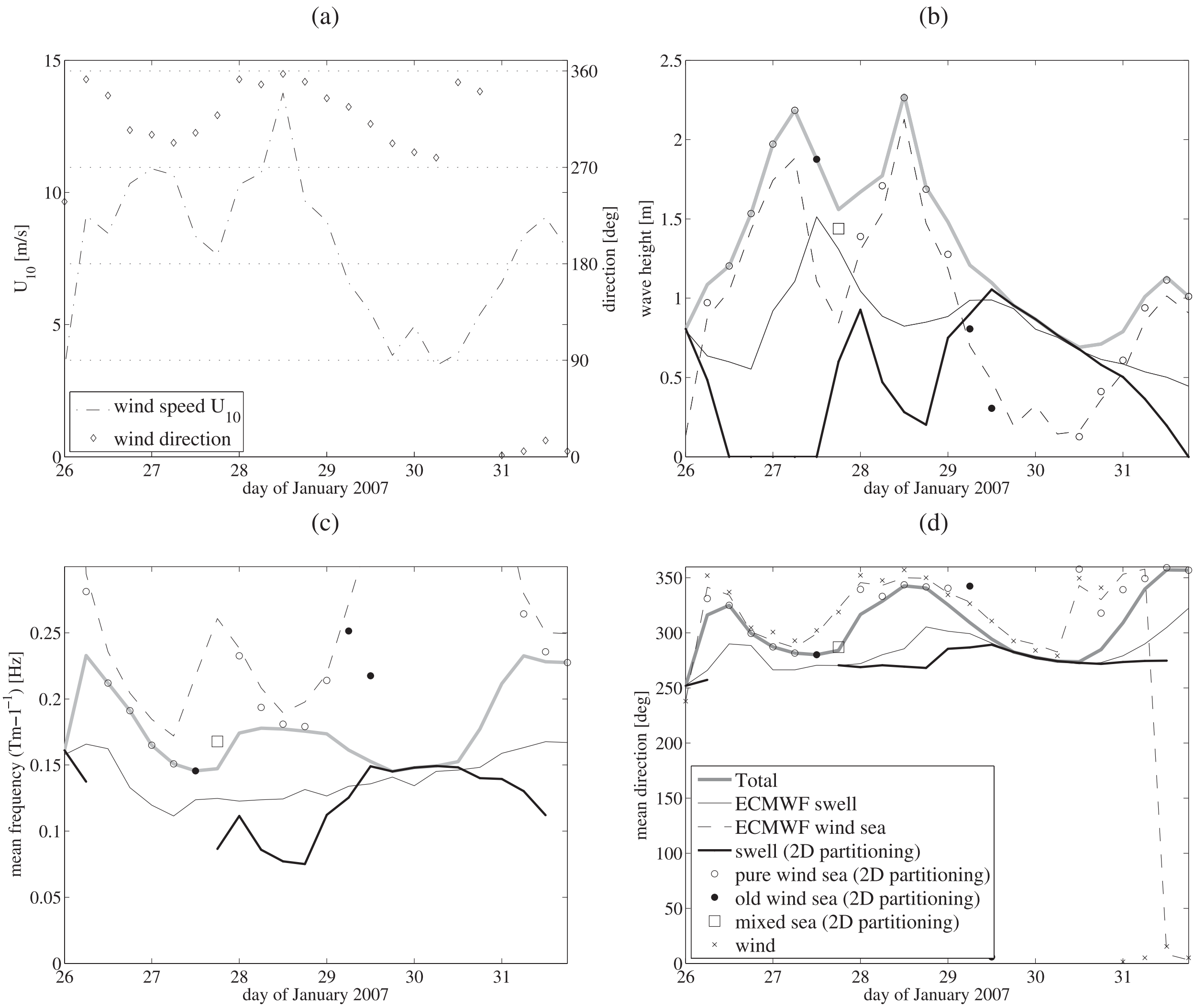

FIG. 6. Wind and wave characteristics from the ECMWF MARS archive (WAM) at Westhinder in the southern North Sea (51.50°N, 2.50°E) from 0000 UTC 26 Jan 2007 to 1800 UTC 31 Jan 2007. (a) Wind speed and direction, (b) significant wave height, (c) mean wave frequency (Tm^{-1}), and (d) mean wave direction. (b)–(d) The entire spectrum (gray thick line), the ECMWF swell estimates (thin black line), the ECMWF wind sea estimates (dash line), of swell estimates using 2D partitioning (thin black dot-marked line), pure wind sea estimates using 2D partitioning (white circles), old wind sea estimates using 2D partitioning (black circles), and mixed wind sea estimates using 2D partitioning (squares).

To analyze these differences, wave spectra from the swell system of 1200 UTC 28 January are shown in Fig. 7. Figure 7a suggests that part of the spectrum is wind sea and part is swell, while partitioning indicates that the spectrum is composed of a single (old wind sea) system. There is little change in Fig. 7b with respect to Fig. 7a, while Fig. 7e shows that some energy of the previously old wind sea system was transferred to lower frequencies forming a second (swell) system. The old wind sea part in Fig. 7d has now (Fig. 7e) become a mixed wind sea due to the rotating wind from 300° over 320° to 350°. In Fig. 7c, the ECMWF swell part is composed of the low-frequency wave system plus a significant part of the higher-frequency system, while in Fig. 7f the more natural (morphological) decomposition into two wave systems is kept in a consistent manner.

b. Wind sea–swell identification using 1D spectrum only

A simple method often used in practice to identify wind sea and swell, because of the sensitivity of ships to large period waves, is to set a constant splitting frequency or period (i.e., 10 s). Although this method might be reliable in zones where wind sea and swell occur markedly separated in the frequency domain, in many circumstances this method is not consistent because frequency

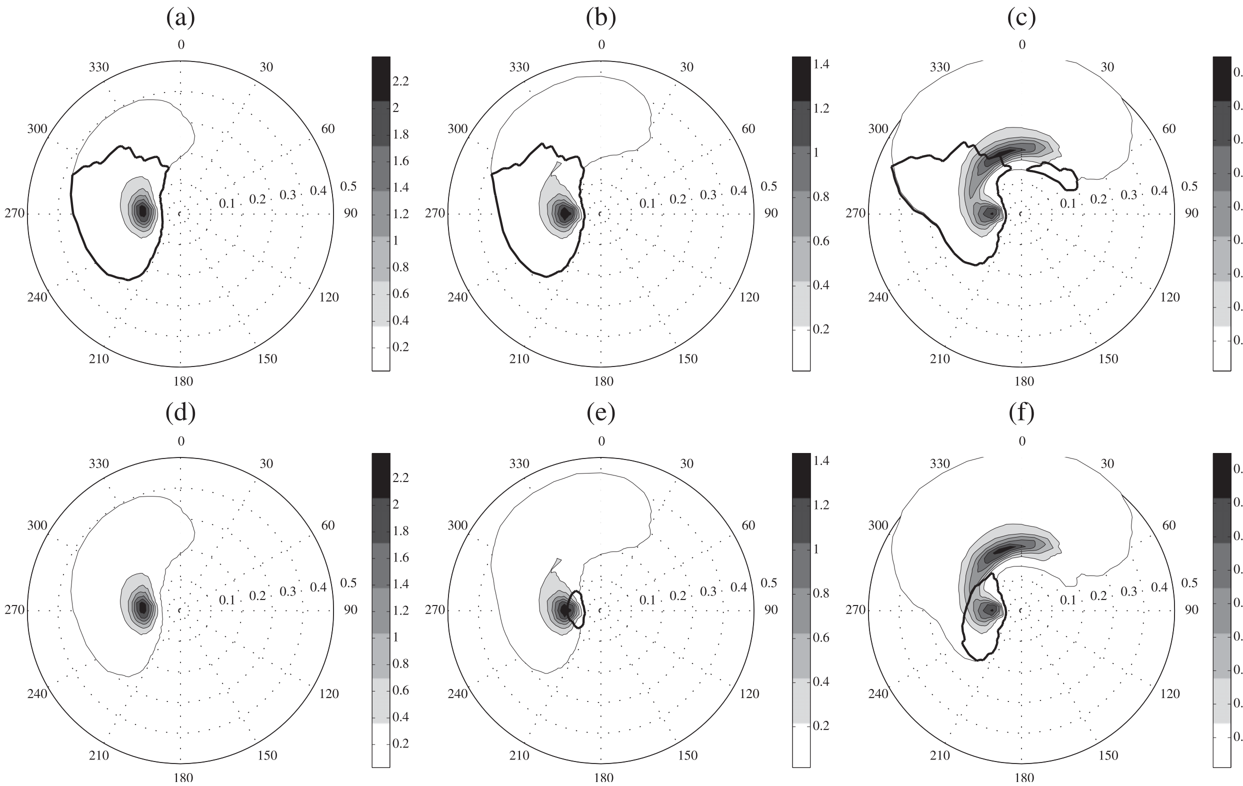

FIG. 7. Wave spectra from ECMWF MARS archive (WAM) at Westhinder (51.50°N, 2.50°E): (a), (d) at 1200 UTC 27 Jan 2007; (b), (e) at 1800 UTC 27 Jan 2007; and (c), (f) at 0000 UTC 28 Jan 2007. (a), (b), and (c) The swell part is contoured (thick continuous line) for ECMWF swell estimates. (d), (e), and (f) For swell estimates using 2D partitioning.

as such does not determine whether a wave system can be considered wind sea or swell.

Another common practice is to split the spectrum close to the peak frequency of the Pierson-Moskowitz (PM) spectrum (1964):

$$f_{\mathrm{PM}} = 0.13\frac{g}{U_{10}}. \tag{3}$$

A factor of 0.8 is commonly applied to indicate the splitting frequency ($f_s = 0.8 f_{\mathrm{PM}}$) to account for uncertainties in the actual sea state or in the angular shift between wind and waves (Earl 1984; Quentin 2002).

Wang and Hwang (2001) use a splitting frequency f_s based on wave steepness. They define the wave mean steepness as

$$\alpha(f_*) = \frac{8\pi\left[\int_{f_*}^{f_{\max}} f^2 S(f)df\right]}{g\left[\int_{f_*}^{f_{\max}} S(f)df\right]^{1/2}}, \tag{4}$$

where $\alpha(f_*)$ is the steepness function at frequency f_*, $S(f)$ is the 1D spectrum, f is frequency, $f_{\max}$ is the upper-frequency limit of the spectrum, and g is the acceleration due to gravity. Because of the f^2 in the formula, the mean wave steepness is more related to the higher-frequency waves and is less affected by lower-frequency waves.

Wang and Hwang (2001) evaluated this steepness function for the PM spectrum at different wind speeds and found that the peak frequency of the steepness function f_m can be related to the wind speed U through the regression equation $U = 0.379 f_m{}^{-1.746}$. The separation frequency (f_s) was then set at the frequency where the wave phase speed equals the wind speed: $f_s = g/2\pi U$. To disregard the wind speed, these (the regression and separation) equations were combined to obtain an expression for the separation frequency as a function of the peak of the steepness function:

$$f_s = 4.112(f_m)^{1.746}. \tag{5}$$

Violante-Carvalho et al. (2002) proposed to fit a Joint North Sea Wave Atmosphere Program (JONSWAP) spectrum [Hasselmann et al. 1973; Eq. (6)] to the high-frequency spectral components to detect the peak that corresponds best to wind sea. For more complex situations, however, when more than two peaks are present, they extend this criterion by two other conditions: one looks at the wind and wave directional information and the other looks at the equilibrium range parameter α

(Phillips 1958). Fitted α values above 0.001 were considered wind sea:

$$S(f) = \alpha g^2 (2\pi)^{-4} f^{-5} e^{-\frac{5}{4}(f/f_p)^{-4}} \gamma^{e^{-(f-f_p)/2\sigma^2 f_p^2}}, \quad (6)$$

where $S(f)$ is the energy spectrum; f is frequency, α is the Phillips constant; g is the acceleration of gravity; f_p is the peak frequency; γ is the peak enhancement factor; and σ is the spectral width factor, $\sigma = \sigma_a$ if $f < f_p$, and $\sigma = \sigma_b$ if $f > f_p$.

Although another 1D method to consider is that of Voorrips et al. (1997), this method uses both wave directional information and wind information and becomes a sort of 2D. Therefore, it will not be used further here.

1) DISCUSSION

It should be mentioned that methods like those of Wang and Hwang (2001) and the "non-extended version" of the method of Violante-Carvalho et al. (2002) have the advantage of disregarding wind data. Moreover, when dealing with 1D spectra, wind data are of lower value because the wind and wave velocity vectors cannot be compared.

Criteria based on the PM peak might overestimate wind sea, especially in growing wind sea conditions where swell is also present. Consequently, the method of Wang and Hwang (2001) is implicitly affected by the two shortcomings mentioned above, as it implicitly compares wind and wave velocities through a criterion obtained from the PM spectrum.

Gilhousen and Hervey (2001) indicate that the steepness method of Wang and Hwang (2001) overestimates wind sea under certain conditions. They replaced Eq. (5) by $f_s = 0.75 f_m$ and introduced an extra mechanism similar to the one of Eq. (3) to complement the algorithm. This approach has not been considered further here because of the rather arbitrary decision to use the higher of the splitting frequencies calculated from the two criteria used.

Following the methodology of Violante-Carvalho et al. (2002), it was found that fitting a JONSWAP spectrum to the higher-frequency part of a wave system helps to identify the peaks that are correlated to that particular wave system. The first tests using this method showed a rather good agreement compared to the 2D scheme (section 3a). Unfortunately, the fitting criterion by itself is not sufficient to decide what is wind sea and what is swell. Therefore, a criterion related to the magnitude of the fitting parameter γ is introduced in the next section.

2) PROPOSED 1D IDENTIFICATION ALGORITHM

In the JONSWAP formulation [Eq. (6)] the peak enhancement factor γ says that the spectrum is sharper than the PM spectrum at the peak frequency, which is considered to be an indication of active wave growth. The Phillips constant α was also found to depend on wind and wave conditions (Hasselmann et al. 1973). However, assuming that the energy at the peak frequency of a swell system cannot be higher than the value of a PM spectrum with the same peak frequency (i.e., α is fixed to its PM value, $\alpha_{PM} = 0.0081$), a simple 1D identification algorithm is set up as follows:

- the ratio (γ^*) between the peak energy of a wave system and the energy of a PM spectrum at the same peak frequency [Eq. (6) with $\gamma = 1$, $f = f_p$ and $\alpha = \alpha_{PM} = 0.0081$] is calculated; and
- if γ^* is above a threshold value ($\gamma^* > 1.0$), the wave system is considered wind sea; otherwise, it is considered swell.

Note that in fact the spectrum no longer needs to be fitted. This criterion was tested here showing good agreement with the results of the 2D scheme. In the following sections, two rather different situations are considered to illustrate the operation of different identification methods.

3) EXAMPLE 4

The dataset of this example corresponds to buoy measurements from the Gulf of Tehuantepec, on the southern Mexican coast at the Pacific Ocean (16°N, 95°W), taken at about 30 km offshore (García 2006). The relevant feature there is a particular combination of meteorological and wave conditions. Due to a geographical depression in the mountain range that crosses the isthmus, a particular wind system, "Tehuanos," is formed. Tehuanos winds blow offshore, generating fetch-limited northerly wind sea in a region where the wave climate is to a great extent characterized by open ocean southerly swells. As a consequence, during Tehuanos wind events, wind sea and swell systems are very distinct in the wave spectra both in frequency and direction. The period considered here goes from 2322 UTC 3 March 2005 to 1651 UTC 5 March 2005 (Fig. 8). The 1D wave energy spectra are shown in Fig. 9.

From Fig. 9 it is clear that these spectra can be split conveniently (at a rather constant frequency) at the trough of the two systems (around 0.15 Hz). Thus, the wave systems present in the spectra are known. Three wind sea and swell identification methods have been applied to these spectra, namely, Wang and Hwang

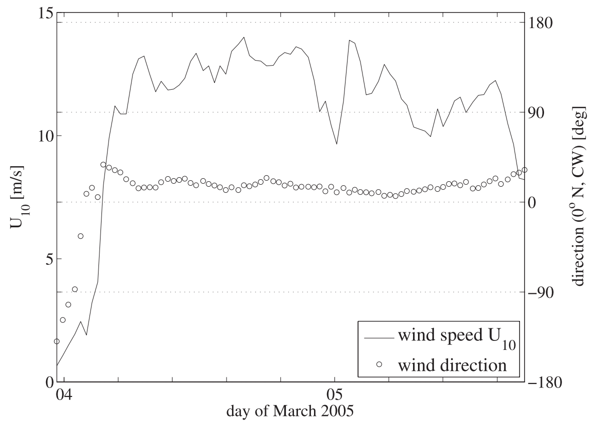

FIG. 8. Wind conditions at the Gulf of Tehuantepec (16°N, 95°W) on the southern Mexican Pacific coast for the period from 2322 UTC 3 Mar 2005 to 1651 UTC 5 Mar 2005.

(2001) method [Eqs. (4) and (5)], the PM peak [Eq. (3)], and the method described here (section 3b).

The separation frequencies from these methods were plotted on top of the time series of 1D spectra. By looking at the gray levels in Fig. 10, the wind sea and swell systems can be clearly discerned. In these conditions, the separation frequency according to the steepness method of Wang and Hwang 2001 (dash line) is systematically at higher frequencies than the splitting frequency (0.15 Hz) which, consequently, results in swell overestimation. The PM peak frequency (dashed–dotted line) is systematically at lower frequencies than the splitting frequency (0.15 Hz), but it seems rather consistent. Note that using factors lower than one would bring the separation frequencies to even lower values, causing more overestimation of wind sea. With the implementation given in this study (section 3b), the separation of the systems (continuous line) is very consistent. Actually, the partitioning of these spectra results in a very clean detection of the two main systems. Regarding the γ^* values of the wave systems, factors corresponding to the swell partitions are in any case lower than 1.0, while γ factors corresponding to wind sea are above 3.

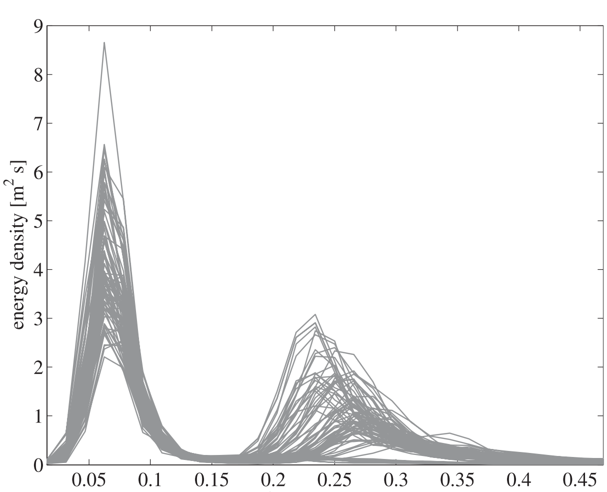

FIG. 9. Wave spectra obtained at the Gulf of Tehuantepec (16°N, 95°W) for the period from 2322 UTC 3 Mar 2005 to 1651 UTC 5 Mar 2005. Spectra are given every 30 min (gray lines).

To analyze details, the spectrum at 2100 UTC 4 March 2005 is shown in Fig. 11. The separation frequencies using these three methods are also indicated. The main features observed in the time series are also visible in the spectrum. According to the method of Wang and Hwang (2001), the wind sea portion only takes part of the tail of the actual wind sea component (dash line). The PM peak frequency corresponding to the present wind conditions (i.e., $U_{10} = 13.5$ m s^{-1}) is 0.1 Hz, taking part of the tail of the swell system as wind sea (dashed–dotted line). With the 1D scheme outlined here (section 3b), two peaks are detected by partitioning. The limit of the two partitions is indicated (filled diamond). The PM spectra corresponding to the two main wave systems are also indicated (dot line). In the case of the swell system, the peak of the PM spectrum has a larger magnitude than the observed swell system ($\gamma^* = 0.0306$), while the peak of the wind sea has a larger magnitude than a PM spectrum at that peak ($\gamma^* = 14.3644$). Note that using partitioning in combination with the PM peak frequency would yield results very similar to those obtained looking at the value of γ^*, but the associated disadvantage is the need of wind speed.

4) EXAMPLE 5

The present dataset was measured by a directional Waverider buoy at Westhinder in the southern North Sea (51.38°N, 2.44°W), where wave conditions are characterized by the presence of local wind sea and occasional swells coming from the north. Wind sea and swell were present in the period from 0030 UTC 12 October 1997 to 1830 UTC 15 October 1997, which is a period of moderate winds in turning wind conditions (Fig. 12).

Contrary to the previous example, the wave systems in this case are not markedly separated. The spectra are rather complex, and the splitting and identification procedures become more complex as well. Moreover, the true systems are not known. Therefore, in this case estimates of the true systems are obtained from the 2D scheme (section 3a). The 2D spectra were reconstructed from spectra of energy, mean direction, and directional spread following Kuik et al. (1988).

Time series of significant wave height of the whole spectrum (thick gray line) and of swell estimates of the

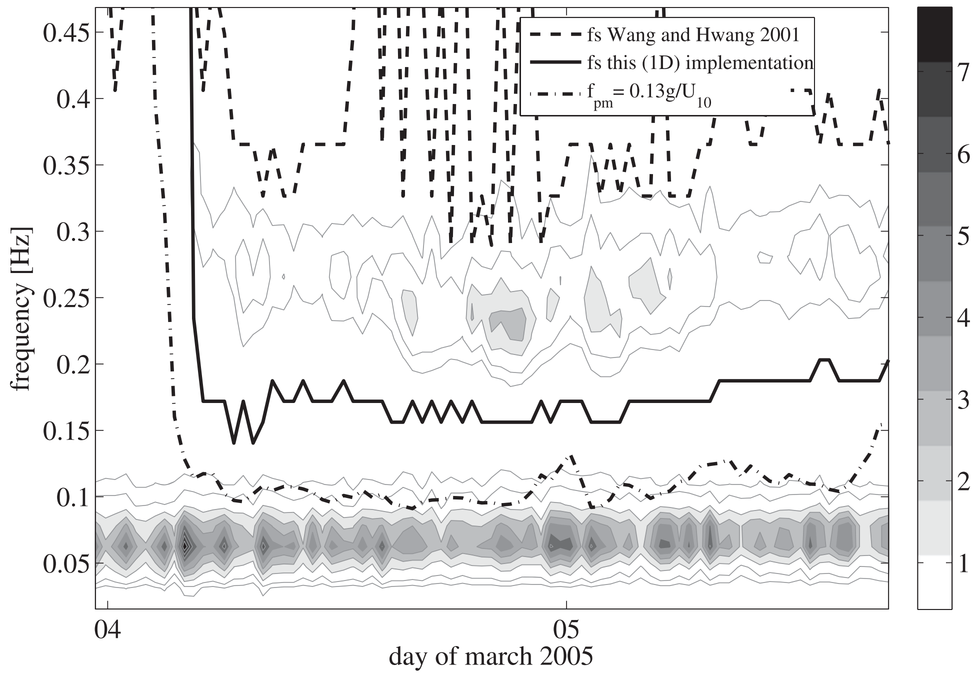

FIG. 10. Time series of 1D energy density spectra (gray levels) obtained at the Gulf of Tehuantepec (16°N, 95°W) for the period from 2322 UTC 3 Mar 2005 to 1651 UTC 5 Mar 2005. And wind sea–swell separation frequencies obtained using the Wang and Hwang (2001) method (thick dashed line), the 1D method proposed in this study (thick continuous line), and the PM peak frequency (thick dashd–dotted line).

2D and three 1D identification methods used in the previous example are shown in Fig. 13.

In Fig. 13 it can be seen that the results of the 1D method given here (section 3b, continuous thick black line) are in good agreement with the results of the 2D scheme (section 3a, continuous circle-marked thin black line). The method of Wang and Hwang 2001 (star-marked dashed line) provides similar estimates in cases in which swell is dominant and there is little or no wind sea (period around the 0000 UTC 13 October 1997 and period after the 1200 UTC 14 October 1997). In periods of wind sea, this method systematically overestimates swell. There is rather good agreement using the PM peak-frequency method (diamond-marked dashed–dotted line),

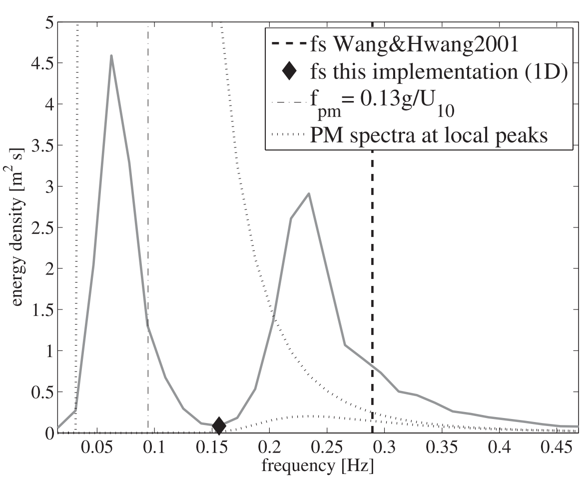

FIG. 11. Wave spectrum from the Gulf of Tehuantepec (16°N, 95°W) at 2100 UTC 4 Mar 2005 and separation frequencies using the Wang and Hwang (2001) method (thick dashed line), the 1D wind sea–swell identification method propose in this study (black diamond), and the frequency of the PM peak (thick dashed–dotted line). The PM spectra corresponding to the two main local peaks (dot lines) are also indicated.

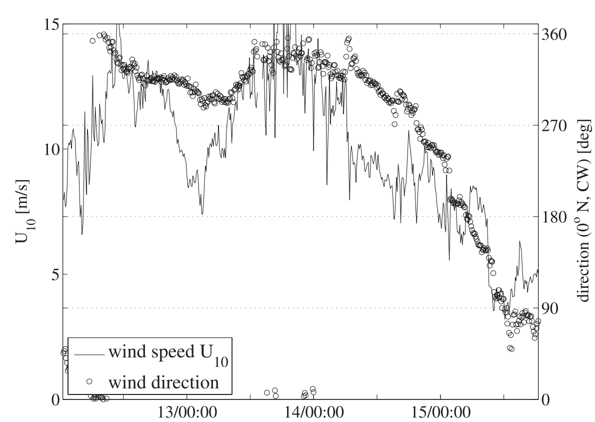

FIG. 12. Wind conditions at Westhinder (51.38°N, 2.44°W) in the southern North Sea for the period from 0030 UTC 12 Oct 1997 to 1830 UTC 15 Oct 1997.

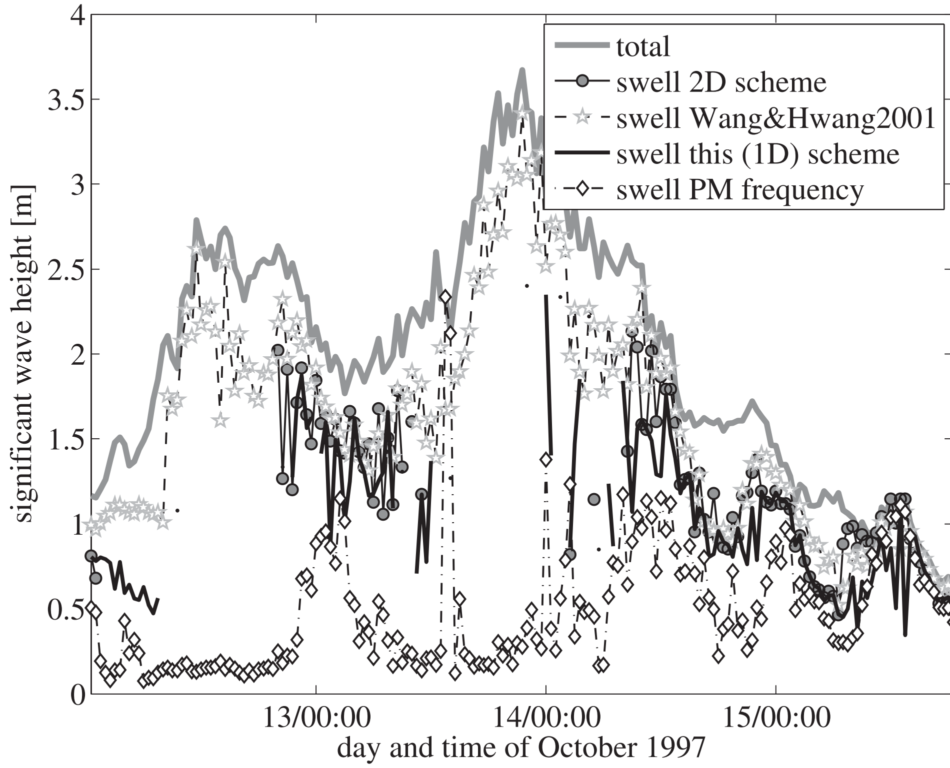

FIG. 13. Time series of significant wave height at Westhinder (51.38°N, 2.44°W) for the period from 0030 UTC 12 Oct 1997 to 1830 UTC 15 Oct 1997 and swell estimates: using the Wang and Hwang (2001) method (star-marked dashed line), the 1D wind sea–swell identification method proposed in this study (thick continuous black line), the PM peak frequency (dashed–dotted diamond-marked line), and the 2D scheme outlined in this study (thin continuous circle-marked line).

especially in the swell-dominated period after 0000 UTC 15 October 1997, but in general this method tends to underestimate swell in typical swell periods.

To analyze the schemes in more detail, the spectrum at 0000 UTC 15 October 1997 is shown in Fig. 14, from where it can be seen that the steepness method splits the spectrum somewhere at the tail of the wind sea component, underestimating wind sea, while the PM peak frequency tends to be at lower frequencies than those obtained for the 2D scheme, resulting in wind sea overestimation. The 1D scheme presented here (section 3b) splits the spectrum more consistently, because of the use of the partitioning step. The values of γ^* for the two main peaks in the present example are 0.27 and 5.52, respectively.

In general, the trends are similar to those from the previous example.

4. Conclusions

Different spectral partitioning techniques have been investigated, emphasizing the fact that the varied existing methods differ mainly in the way they assess whether partitions are significant, which implies basically the use of different combining strategies. It was found that the current mechanisms used for combining partitions reported in the literature are not very robust. Moreover, they demand the use of arbitrary parameterizations. As a consequence, the existing spectral partitioning methods deliver rather inconsistent output for wave systems.

The introduction of an image-processing tool based on a 2D low-pass-filtering step aiming to reduce noise was found to improve the robustness of the 2D partitioning scheme considerably. The detection of wave systems is more consistent, and the method is not very sensitive to parameter value settings.

Also, a more robust partitioning scheme for 1D spectra has been proposed. The method aims to remove the most obvious spurious peaks. The criteria used for this purpose proved to be sufficient to reduce the number of partitions to a reasonable value.

Wind sea and swell can be identified from looking at different environmental and physical characteristics of wave systems. However, results from different methods reported in the literature sometimes differ largely.

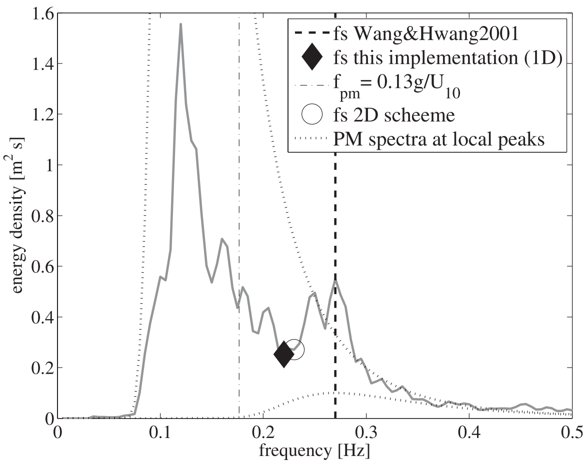

FIG. 14. Wave spectrum at Westhinder (51.38°N, 2.44°W) at 0000 UTC 15 Oct 1997 and separation frequencies using the Wang and Hwang (2001) method (thick dashed line), the 1D wind sea–swell identification method proposed in this study (black diamond), the frequency of the PM peak (thick dashed–dotted line), and the 2D scheme presented here (empty circle). The PM spectra corresponding to the two main local peaks (dotted curves) are also indicated.

For the identification of wind sea and swell using the 2D spectrum plus wind speed and direction, a wind wave generation mechanism in combination with 2D partitioning uses all available information and gives the most consistent estimates.

Regarding the 1D wind sea–swell identification methods, it is pointed out that the method of Wang and Hwang (2001) used at the NDBC tends to overestimate swell, especially during wind sea periods. The PM peak-frequency method is more consistent but underestimates swell systematically. Quite consistent results were achieved using 1D spectra only, by looking at the ratio (γ^*) between the energy at the spectral peak of a partition and the energy at the peak of a PM spectrum with the same peak frequency.

The identification of wind sea and swell both in the 2D and 1D spectra is found more consistent in combination with partitioning.

Acknowledgments. J. Portilla acknowledges scholarship funding from the Flemish Interuniversity Council (VLIR) and from the Research Foundation Flanders Funds G.0477.07. Buoy data from Westhinder were obtained from Guido Dumon of the Agency for Maritime and Coastal Services of the Ministry of Transport and Public Works, data from buoy 41013 were downloaded from the NDBC Web site, and data from the Gulf of Tehuantepec were measured by CICESE Wave Group during the intOA Experiment Field Campaign (CONACYT 62520 dirocIOA; SEP-2003-002-44718 intOA). ECMWF data were obtained in the framework of the EU project SEAMOCS (Contract MRTN-CT-2005-019374). The research benefited from close collaboration with colleagues in the Belgian Science Policy Project QUEST4D. The authors thank the anonymous reviewers for their dedicated and constructive comments.

REFERENCES

Aarnes, J. E., and H. E. Krogstad, 2001: Partitioning sequences for the dissection of directional ocean wave spectra: A review. Tech. Rep. Work Package 4 (Wp4) of the EnviWave (EVG-2001-00017) Research Program, EU Energy, Environment and Sustainable Development Program, 23 pp.

Bidlot, J. R., 2001: ECMWF wave-model products. *ECMWF Newsletter*, No. 91, ECMWF, Reading, United Kingdom, 9–15.

Brüning, C., S. Hasselmann, K. Hasselmann, S. Lehner, and T. W. Gerling, 1994: First evaluation of ERS-1 synthetic aperture radar wave mode data. *Global Atmos. Ocean Syst.,* **2,** 61–98.

Donelan, M., J. Hamilton, and W. Hui, 1985: Directional spectra of wind-generated waves. *Philos. Trans. Roy. Soc. London,* **315,** 509–562.

Drennan, W. M., H. C. Graber, D. Hauser, and C. Quentin, 2003: On the wave age dependence of wind stress over pure wind seas. *J. Geophys. Res.,* **108,** 8062, doi:10.1029/2000JC000715.

Earl, M. D., 1984: Development of algorithms for separation of sea and swell. National Data Buoy Center Tech. Rep. MEC-87-1, NDBC, 53 pp.

García, N. H., 2006: Evaluación del flujo de momento entre la atmósfera y el océano bajo diferentes condiciones de oleaje (in Spanish). M.S. thesis, CICESE Mexico, 74 pp.

Gerling, T. W., 1992: Partitioning sequences and arrays of directional ocean wave spectra into component wave systems. *J. Atmos. Oceanic Technol.,* **9,** 444–458.

Gilhousen, D. B., and R. Hervey, 2001: Improved estimates of swell from moored buoys. *Proc. Fourth Int. Symp. WAVES 200*, Alexandria, VA, ASCE, 387–393.

Hanson, J. L., and O. M. Phillips, 2001: Automated analysis of ocean surface directional wave spectra. *J. Atmos. Oceanic Technol.,* **18,** 277–293.

Hasselmann, K., and Coauthors, 1973: Measurement of wind-wave growth and swell decay during the Joint North Sea Wave Project (JONSWAP). *Dtsch. Hydrogr. Z.,* **12,** 7–95.

Hasselmann, S., K. Hasselmann, and C. Brüning, 1994: Extraction of wave spectra from SAR image spectra. *Dynamics and Modelling of Ocean Waves*, G. J. Komen et al., Eds., Cambridge University Press, 391–401.

——, C. Brüning, K. Hasselmann, and P. Heimbach, 1996: An improved algorithm for retrieval of ocean wave spectra from synthetic aperture radar image spectra. *J. Geophys. Res.,* **101,** 16 615–16 629.

Holthuijsen, L. H., 2007: *Waves in Oceanic and Coastal Waters*. Cambridge University Press, 387 pp.

Janssen, P. A. E. M., 1991: Quasi-linear theory of wind wave generation applied to wave forecasting. *J. Phys. Oceanogr.,* **21,** 1631–1642.

Komen, G. J., S. Hasselmann, and K. Hasselmann, 1984: On the existence of a fully developed wind–sea spectrum. *J. Phys. Oceanogr.,* **14,** 1271–1285.

——, L. Cavaleri, M. Donelan, K. Hasselmann, S. Hasselmann, and P. A. E. M. Janssen, Eds., 1994: *Dynamics and Modelling of Ocean Waves*. Cambridge University Press, 532 pp.

Kuik, A. J., G. P. Van Vledder, and L. H. Holthuijsen, 1988: A method for the routine analysis of pitch-and-roll buoy wave data. *J. Phys. Oceanogr.,* **18,** 1020–1034.

Lionello, P., H. Günter, and P. A. E. M. Janssen, 1992: Assimilation of altimeter data in a global third-generation wave model. *J. Geophys. Res.,* **97,** 453–474.

Phillips, O. M., 1958: The equilibrium range in the spectrum of wind-generated waves. *J. Fluid Mech.,* **4,** 426–434.

——, 1985: Spectral and statistical properties of the equilibrium range in wind-generated gravity waves. *J. Fluid Mech.,* **156,** 505–531.

Pierson, J. W., and L. Moskowitz, 1964: A proposed spectral form for fully developed wind seas based on the similarity theory of S. A. Kitaigorodskii. *J. Geophys. Res.,* **69,** 5181–5190.

Quentin, C., 2002: Etude de la surface océanique, de sa signature radar et de ses interactions avec le flux turbulent de quantité de mouvement dans le cadre de l'expérience FETCH (in French). Ph.D. thesis, Université de Paris, 263 pp.

Rodríguez, G., and C. Guedes Soares, 1999: A criterion for the automatic identification of multimodal sea wave spectra. *Appl. Ocean Res.,* **21,** 329–333.

Thomas, J., 1988: Retrieval of energy spectra from measured data for assimilation into a wave model. *Quart. J. Roy. Meteor. Soc.,* **114,** 781–800.

Violante-Carvalho, N., C. E. Parente, I. S. Robinson, and L. M. P. Nunes, 2002: On the growth of wind generated waves in a swell dominated region in the South Atlantic. *J. Offshore Mech. Arctic Eng.,* **124,** 14–21.

Voorrips, A. C., V. K. Makin, and S. Hasselmann, 1997: Assimilation of wave spectra from pitch-and-roll buoys in a North Sea wave model. *J. Geophys. Res.,* **102,** 5829–5849.

Wang, D. W., and P. A. Hwang, 2001: An operational method for separating wind sea and swell from ocean wave spectra. *J. Atmos. Oceanic Technol.,* **18,** 2052–2062.

Young, I. R., and T. J. Glowacki, 1996: Assimilation of altimeter wave height data into a spectral wave model using statistical interpolation. *Ocean Eng.,* **23,** 667–689.